ISSN 0006-2979, Biochemistry (Moscow), 2006, Vol. 71, No. 5, pp. 505-512. © Pleiades Publishing, Inc., 2006.
Original Russian Text © M. Malisauskas, A. Darinskas, V. V. Zamotin, A. Gharibyan, I. A. Kostanyan, L. A. Morozova-Roche, 2006, published in Biokhimiya, 2006, Vol. 71, No. 5, pp. 626-635.
Originally published in Biochemistry (Moscow) On-Line Papers in Press, as Manuscript BM05-230, February 19, 2006.

Intermediate Amyloid Oligomers of Lysozyme: Is Their Cytotoxicity a Particular Case or General Rule for Amyloid?

M. Malisauskas[1], A. Darinskas[2], V. V. Zamotin[1], A. Gharibyan[1], I. A. Kostanyan[3], and L. A. Morozova-Roche[1,4]*

[1]*Department of Medical Biochemistry and Biophysics, Umea University, Umea 90187, Sweden; E-mail: mantas.malisauskas@medchem.umu.se*
[2]*Laboratory of Pharmacology, Institute of Immunology, Vilnius University, Moletu st. 29, Vilnius, 08409 Lithuania; E-mail: innovita@innovitaresearch.org*
[3]*Shemyakin and Ovchinnikov Institute of Bioorganic Chemistry, Russian Academy of Sciences, ul. Miklukho-Maklaya 16/10, 117997 Moscow, Russia; E-mail: iakost@mail.ibch.ru*
[4]*Institute of Biological Instrumentation, Russian Academy of Sciences, ul. Institutskaya 7, 142290 Pushchino, Moscow Region, Russia; E-mail: ludmilla.morozova-roche@medchem.umu.se*

Received October 17, 2005

Abstract—In the current study we investigated the molecular mechanisms of cytotoxicity of amyloid oligomers of horse milk lysozyme. We have shown that lysozyme forms soluble amyloid oligomers and protofibrils during incubation at pH 2.0 and 4.5 and 57°C. These structures bind the amyloid-specific dyes thioflavin T and Congo Red, and their morphology and size were analyzed by atomic force microscopy. Monomeric lysozyme and its fibrils did not affect the viability of three cell types used in our experiments including primary murine neurons and fibroblasts, as well as neuroblastoma cell line IMR-32. However, soluble amyloid oligomers of lysozyme caused death of all these cell types, as estimated by flow-cytometry counting dead cells stained with ethidium bromide. The primary cell cultures appeared to be more sensitive to amyloid than neuroblastoma cell line IMR-32. Amyloid cytotoxicity depends on the size of oligomeric particles: samples containing 20-mers formed at pH 4.5 were more toxic than tetramers and octamers present in the solution at pH 2.0. Soluble amyloid oligomers can self-assemble into doughnut-like structures; however, no correlation was observed between the amount of the doughnut-like structures in the sample and its cytotoxicity. The fact that the intermediate oligomers of such an abundant protein as lysozyme display cytotoxicity confirms a hypothesis that cytotoxicity is a common feature of protein amyloid. Inhibition of intermediate oligomer formation is crucial in preventing amyloid pathogeneses.

DOI: 10.1134/S0006297906050063

Key words: amyloid, atomic force microscopy, cytotoxicity, apoptosis, oligomer

Molecular mechanisms of pathological processes associated with formation and accumulation of amyloid aggregates in various organs and tissues in amyloid diseases, such as Alzheimer's and Parkinson's diseases, type II diabetes, hereditary amyloid polyneuropathies, etc. remain a central theme in modern research [1-5]. Many observations show tissue damage and cell death resulting from amyloid formation. At the same time, it is obvious that in various amyloid diseases the amount of amyloid deposits can vary over a very wide range, i.e. from milligrams to kilograms. The latter is characteristic, for instance, of lysozyme amyloid agglomeration in liver of patients suffering from systemic amyloidosis [6, 7]. However, there is no direct association between amyloid amount and severity of pathological process in neurodegenerative disorders such as Alzheimer's disease. Some data indicate that amyloid deposits may not achieve significant level in brain of Alzheimer's patients with progressive amnesia and all symptoms of neurodegeneration, whereas the level of soluble amyloid oligomers in the brain is greatly elevated [8, 9].

Studies on cytotoxicity of amyloid structures are actively conducted with the use of many natural proteins, both involved in pathogenesis and forming amyloid *in vitro* [9-12]. Amyloid structures known to date have com-

Abbreviations: AFM) atomic force microscopy.

* To whom correspondence should be addressed.

mon features, such as formation of β-sheeted fibrillar core, allowing their affiliation into one general group [13]. These observations have led to a hypothesis on common functional properties of amyloid fibrils and, hence, on common mechanisms of amyloid cytotoxicity [11]. Some data are indicative of particular cytotoxicity, both *in vivo* and *in vitro*, of prefibrillar aggregates [9-12]. Prefibrillar structures of proteins unrelated to clinical amyloidoses, such as α-lactalbumin [12], SH3 domain, and HypF-N protein [11], are cytotoxic, whereas mature fibrils of the same proteins and pathology-associated fibrils of Aβ peptide and transthyritin are not cytotoxic [10, 11]. However, because of significant heterogeneity of amyloid structures observed within the same protein specimen and the vague definition of prefibrillar structures, it remains unclear what type of amyloid structures is toxic and whether the cell death caused by amyloid occurs via a specific molecular mechanism or amyloid leads to mere physical damage of cell structures.

A goal of our study was investigation of cytotoxic properties of amyloid structures of horse lysozyme, a protein which is found in many organs and tissue liquids, in particular, in mare's milk. Lysozyme, whose concentration in mare's milk reaches hundreds of milligrams per liter, plays an important role in body defense from external bacterial infections [14]. The fermented milk, koumiss, is widely used as a beverage possessing healing qualities. Horse lysozyme is also a model protein in studies on protein structure and general principles of protein folding [15-17]. It belongs to a large family of structurally homologous proteins encompassing both lysozymes and α-lactalbumins. Horse lysozyme takes a particular place among these proteins because it combines structural characteristics and folding properties of both families (Fig. 1) [15-18]. Horse lysozyme possesses bacteriolytic activity of traditional lysozymes, but, unlike egg white lysozyme, it contains a calcium-binding site similar to the α-lactalbumin site. For this reason, horse lysozyme was suggested to be an evolutionary bridge between these two families [15, 18].

Fig. 1. Scheme for the horse lysozyme molecule produced using RasMol software.

Note that the members of lysozyme/α-lactalbumin family are amyloidogenic. In the 1990s, mutant forms of human lysozyme were found to be a cause of systemic amyloidoses [6, 7]. Human lysozyme can also form amyloid fibrils *in vitro*, which are indistinguishable, both structurally and morphologically, from amyloid structures associated with diseases [19]. Although human α-lactalbumin forms mature fibrils [20, 21], its oligomeric structures were found toxic for both immature and tumor cells [12]. Recently, we have shown that unlike traditional lysozymes and α-lactalbumins [19-21], horse lysozyme forms both short linear protofilaments, which do not achieve the length of mature fibrils (of microns) and closed rings. The number of rings and their size depend on the concentration of calcium ions and pH of the solution [22]. The study of cytotoxic properties of ring amyloid structures is of particular importance, because the amyloid rings of Aβ peptide and α-synuclein inducing neuronal death have been recently proposed to play the key role in pathogeneses of Alzheimer's and Parkinson's diseases [23]. In the present study, soluble amyloid oligomers of horse lysozyme have been obtained under conditions of fibril formation, before the formation of filament structures, and their toxicity was measured in comparison with that of monomeric protein and fibrils. The direct dependence between the toxic properties of amyloid oligomers and their size is shown.

MATERIALS AND METHODS

Protein samples. Horse lysozyme was isolated from horse milk as described previously [24]. Protein concentration was determined on a Beckman (USA) UV-VIS spectrophotometer using extinction coefficient $E_{1\%}$ = 23.5 at wavelength 280 nm [24]. To produce amyloid structures, lysozyme at concentration of 20 mg/ml (1.36 mM) was incubated in 20 mM glycine buffer, pH 2.0, or in 10 mM sodium acetate buffer, pH 4.5, in the presence of 0.2% sodium azide at 57°C, as described previously [22].

Interaction of amyloid samples with thioflavin T and Congo Red. Experiments on thioflavin T binding were carried out according to a modification of the method of Levine [25]. Fluorescence spectra of thioflavin T were

registered using a FluoroMax-2 spectrofluorimeter (JOBIN YVON/PSEX Instruments, USA) within the range of wavelengths 450-550 nm; the excitation wavelength was 440 nm and slit width was 5 nm. Fresh stock solution of 2.5 mM thioflavin T in phosphate buffer containing 10 mM potassium phosphate and 150 mM sodium chloride, pH 7.0, was prepared before every experiment. The solution was filtered through a filter with 0.2-μm pore size. The fluorescence intensity measurements started 4-5 min after the dye addition to protein samples to achieve thermal equilibrium in a quartz cell with 0.2 cm optical path length. The samples were under continuous agitation, and the fluorescence intensity was averaged over 60 sec to increase the signal/noise ratio.

Congo Red binding was determined as described previously [19]. Absorption spectra of the reaction mixture with Congo Red were recorded using the Beckman spectrophotometer.

Atomic force microscopy (AFM). The amyloid structures were imaged on a PicoPlus AFM atomic force microscope (Molecular Imaging, USA) using a scanning device (100 μm range) operating in oscillation mode. Both acoustic and magnet cantilevers were used to achieve high resolution on scanning in air and liquid medium. Both cantilever types were equipped with silicon TESP probes with radius of curvature no more than 10 nm (Digital Instruments, USA). The scanning of samples in acoustic mode was carried out at 1 Hz frequency and resolution of 512 × 512 points. Resonance frequency of probes was within the range of 120-160 kHz. In magnetic mode, the probes were resonant at about 25 kHz. Altitude, amplitude, and phase images were obtained simultaneously. To avoid scanning artifacts, the sample scanning was carried out in direct and reverse motion of the probe. The scanning device was calibrated by measuring the distance of 0.3 Å between atomic layers of pyrolytic graphite on the *z*-scale and using standard 1-μm calibration grid (Molecular Imaging) in the *xy*-plane.

Amyloid samples at concentration of 200 μg/ml were placed on the surface of freshly cleaved mica (GoodFellow, UK) for 5 sec, then washed (3 × 250 μl) with water from a MilliQ (Millipore, USA) and dried at room temperature. The samples were visualized in an open fluid cell at the initial concentration of 50-80 μg/ml of the sample which was incubated for 10 min followed by washing with the incubation buffer (3 × 200 μl); thereafter, 300 μl of the same buffer was added to the cell. The short adsorption time of amyloid structures on the mica surface before the scanning, in comparison with the hours that are necessary to obtain amyloid, in combination with high dilution of the samples, convincingly prove that the amyloid aggregation was not induced by interaction with the mica surface. In control measurements, graphite was used as a substrate as well. Topographic images of amyloid oligomers and fibrils remained the same under all measurement conditions.

Determination of molecular size of amyloid structures. The size of protein structures was measured by combination of serial cross-sections of their height images using the PicoPlus software (Molecular Imaging), as well as Scanning Probe Image Processor-SPIP software (Image Metrology, Denmark). In the latter case, the height of all protein particles was measured; the number of particles varied from 1000 to 4000 per 1 × 1 μm of mica surface. Generally, three or four arbitrary sites were selected, wherein each SPIP measurement was carried out in triplicate. Distributions of *z*-heights of the observed particles were measured using a grain analysis module in the SPIP software. The heights of all structures exceeding the surface threshold at the defined noise level were determined. Due to the adhesion to mica, the protein particles had larger horizontal than vertical sizes. In addition, scanning probes, due to their specific geometry, could also result in broadening of horizontal parameters. To compensate for the influence of the probe, the deconvolution module of the SPIP software was used to ensure that the probe shape does not result in topographical artifacts. Microscopic control samples of known parameters were measured including single-wall nanotubes and latex particles of 1.0 and 1.5 nm diameter, respectively. These measurements confirmed the conclusion of earlier studies [26, 27] that the diameter at half-altitude of a protein particle approximated as a "spherical cup" describes well the effect of horizontal broadening in atomic force microscopy.

Thus, the volume of particles V_{AFM} is described by the equation:

$$V_{AFM} = (\pi h/6)(3r^2 + h^2), \quad (1)$$

where h is height and r is radius of a particle at half-height [20].

The molecular volume of monomeric lysozyme, V_m, was determined by the equation:

$$V_m = (M_o/N_A)(V_1 + dV_2), \quad (2)$$

where M is a protein molecular mass, N_A is Avogadro's number, d is an estimation of protein hydration (0.4 mol H_2O/mol protein), and V_1 and V_2 are specific partial volumes of the protein (0.74 cm^3/g) and water (1 cm^3/g), respectively [27]. The number of lysozyme molecules, n, in oligomeric particle was determined via the ratio:

$$n = V_{AFM}/V_m. \quad (3)$$

Cell cultures. Primary cell cultures including primary neuronal culture consisting of neuronal and glial cells and primary cultures of murine embryonal fibroblasts (PMEF) were isolated from 9-12.5-day murine embryos of BALB/c line by the method described previously [28, 29]. The cells were grown as monolayers in DMEM medium containing 1000 mg/liter D-glucose, 110 mg/

liter sodium pyruvate, 10% fetal serum, 2 mM L-glutamine, and 100 U/ml penicillin/streptomycin (Biological Industries, Israel) at 37°C in an atmosphere of 5% CO_2. The medium was substituted daily during the experiments. The cell line IMR-32 was grown under the same conditions. Viability of the cells was determined after 24 and 48 h incubation in the presence of amyloid structures, because it was shown earlier that hours or even days are necessary for metabolic response to amyloid at the cell level [9-11].

Cell staining with ethidium bromide. The primary cells achieved the continuous-lawn stage in three days after their isolation. They were treated with 0.05% trypsin and 0.53 mM EDTA (Gibco, UK), washed, and aliquots of cell suspension (200 μl) were placed into the wells of 96-well plates (Becton Dickinson, USA), taking 10,000 cells per well. After 24-h incubation, the medium was substituted with a fresh portion containing the previously formed amyloid structures of lysozyme added to the final concentration of 5-50 μM. The incubation buffer and freshly dissolved monomeric lysozyme were taken as controls.

The cells were incubated in the presence of lysozyme amyloid for 48 h; thereafter they were washed from plates as described above and resuspended in the PMEF medium (Gibco). Cell suspension (500 μl) in PMEF medium was stained with 5 μl of 20 mg/ml ethidium bromide (EtBr) for 10 min at 4°C. The number of viable cells was measured on a FACS Caliber flow cytometer (Becton Dickinson) according to the manufacturer's protocol. Viability was evaluated via calculation of 10,000 cases using the Cell Quest software package (FACS Caliber).

RESULTS

Binding of amyloid dyes with protein aggregates. Kinetics of the formation of lysozyme amyloid structures was evaluated via their binding with the fluorescent dye thioflavin T (Fig. 2), which is widely used as a marker of amyloid β-sheet formation [19, 25]. Aliquots of protein specimens were sampled after various incubation times and mixed with a buffer containing thioflavin T. Both lysozyme samples incubated at pH 2.0 and 4.5, 57°C, were characterized by a short lag-phase of 3-5 h, which corresponded to the initiation of molecular self-assembly into oligomeric complexes or initial nuclei [19]. During further incubation, the thioflavin T fluorescence intensity increased, thus corresponding to accumulation of amyloid β-sheets in the solution. The fluorescence curve achieved a plateau corresponding to 10-7.5-fold elevation of fluorescence intensity of the dye as a result of incubation of the lysozyme solution for 120 h at pH 2.0 and 200 h at pH 4.5 (Fig. 2).

Amyloid structures characterized by affinity to thioflavin T were also evaluated with respect to their ability to bind another amyloid dye, Congo Red, which is also specific to β-sheeted amyloid [19, 22]. The time-dependent protein specimens incubated either at pH 2.0 or at pH 4.5 were sampled during the lag-phase, the growth phase (Fig. 2), as well as after achievement of plateau of fluorescence and were mixed with the solutions of Congo Red. In the first case, the absorption spectrum of Congo Red was unchanged; a long-wavelength shift for 2-3 nm in the absorption spectrum of the dye corresponded to the growth phase, and a shift for 5-6 nm corresponded to the plateau on the kinetic curve (data not shown). These alterations show that the formation and growth of amyloid structures result in their affinity to both thioflavin T and Congo Red.

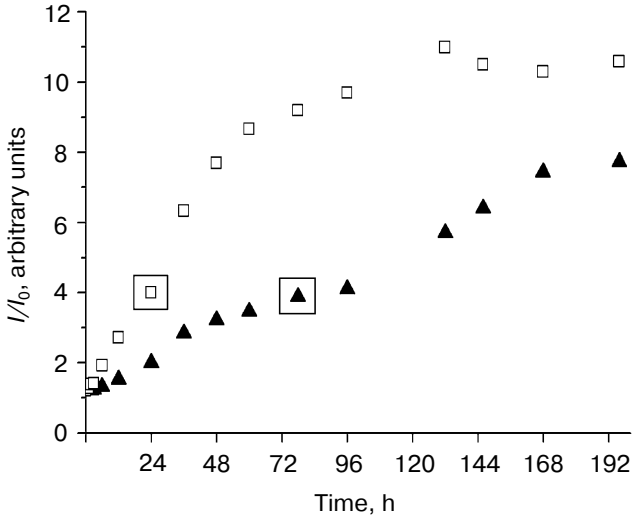

Fig. 2. Kinetics of amyloid formation from horse lysozyme as traced by thioflavin T binding. The sample incubated at pH 4.5 and 57°C is designated with solid triangles and the sample incubated at pH 2.0 and 57°C is designated with empty squares. I/I_o is a relative fluorescence of the dye bound to amyloid structures, where I is a relative fluorescence of the dye bound to amyloid and I_o is intrinsic fluorescence of free dye in solution.

Morphology and stoichiometry of amyloid structures. Further detailed analysis of size and morphology of lysozyme amyloid structures was carried out using atomic force microscopy (AFM). From the moment of the fluorescence enhancement, we observed appearance of spherical particles (Fig. 3a) differing in their height along the *z*-axis and in diameter at half-height in the *xy*-plane. These parameters were measured also using the SPIP grain analysis described above. For further evaluation of cytotoxicity of lysozyme solutions in the process of its incubation, we chose time ranges corresponding to monomer, oligomer, and fibrillar structures. In fresh solution of protein, only monomeric lysozyme was present; its particles were of approximately 0.4 nm height, and calculation of molecular volume of these particles according to Eqs. (1)-(3) showed that the experimental values are in good agreement with the monomer volume (table). The particles increased in size over the course of the protein solu-

tion incubation (Fig. 3a), thus suggesting the oligomerization of monomeric lysozyme.

For detailed analysis we chose 72-h time period for the sample at pH 4.5 and 24-h time period for the sample at pH 2.0, with equal enhancement of thioflavin T fluorescence corresponding to these periods, suggesting the presence of β-sheeted structures in similar amounts. Application of SPIP grain analysis to the protein incubated at pH 2.0 showed that particles of approximately 0.7 and 1.05 nm in height (table) and, respectively, 20-21 and 22-23 nm in diameter at the half-height are present in the sample together with monomeric lysozyme. Control measurements of cross-sections of the particles confirmed these observations. The stoichiometry of these oligomers calculated using Eqs. (1)-(3) showed that they are tetramers and octamers, respectively. There were no larger particles observed in the sample incubated at pH 2.0, whereas fractions of larger particles of approximately 2.03 nm in height were observed in the sample incubated at pH 4.5. These observations were confirmed by SPIP grain analysis as well as by measurements in multiple cross-sections. The latter particles corresponded to protein oligomers composed of >20 monomer molecules. It is worth noting that no fibrillar structure was observed in either protein sample at this incubation stage.

Single-chained fibrillar polymers comprised the main population of protein structures in both samples at the stage corresponding to the plateau on the curve of kinetic dependence of fibril formation (Figs. 2 and 3b). Their height in cross-section was 2 nm, thus evidencing for typical protofilaments observed earlier at pH 4.5 and 57°C in the presence of 10 mM $CaCl_2$ [22]. Their length varied from 30 to 300 nm. Straight and flexible fibrils were present, some of them having smooth edges, whereas others had prominent periodicity along the longitudinal axis, thus endowing them morphology of "beads".

It is notable that ring structures characterized by 4th or 5th order of symmetry (Fig. 3, c and d) were sometimes

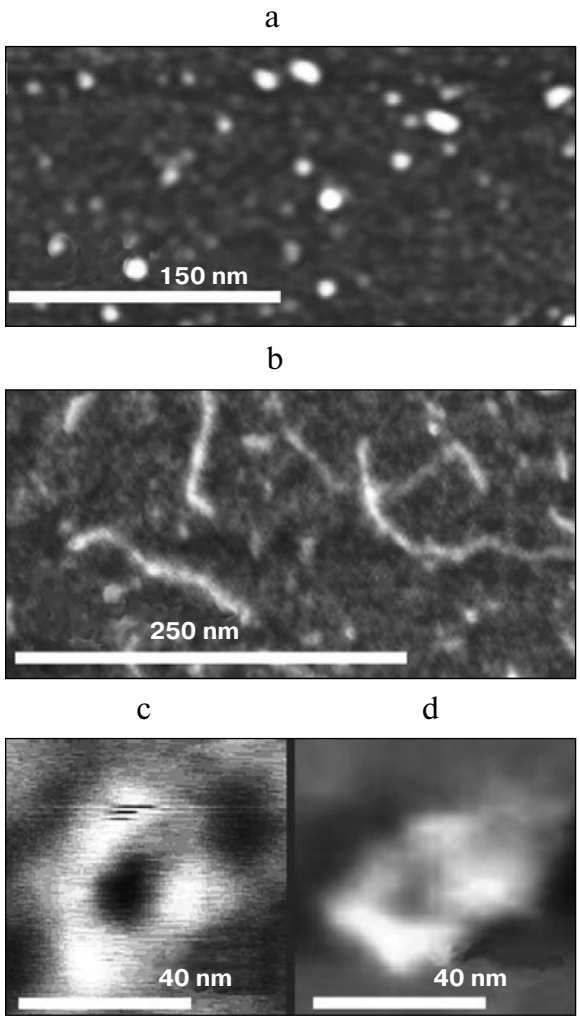

Fig. 3. AFM imaging of amyloid structures of horse lysozyme. a) Amyloid oligomers formed during 72-h incubation at pH 4.5 and 57°C. b) Amyloid protofilaments observed at pH 2.0 after five days of incubation at 57°C. c, d) Amyloid rings formed in both samples at pH 2.0 and 4.5, respectively, in the process of incubation.

Parameters of amyloid oligomers of horse lysozyme evaluated by AFM

Type of oligomers*		Height, nm**	Diameter, nm**	Volume, nm^3**	Number of monomers**	Number of monomers***
pH 4.5	pH 2.0					
0.4	0.4	0.39 ± 0.06	15.7 ± 2.4	38.3 ± 11.6	1 ± 0.5	1 ± 0.5
0.7	0.7	0.70 ± 0.14	20.9 ± 0.8	122.5 ± 9.4	4 ± 0.5	5 ± 2
1.1	1.1	1.05 ± 0.11	22.3 ± 1.4	207.9 ± 26.8	8 ± 1	8 ± 3
2.1	not found	2.03 ± 0.22	27.8 ± 2.8	584.3 ± 119.0	21 ± 4	25 ± 7

* Oligomers identified at two different pH values and classified according to their dimensions.
** Height along *z*-axis and diameter at the half maximal height were determined in the cross-sections of the particles, the volume and stoichiometry of oligomers were calculated using Eqs. (1)-(3).
*** The same parameters were measured by method of grain analysis (SPIP, Denmark) and stoichiometry was calculated by using Eqs. (2) and (3).

observed in both lysozyme samples at growth phase as well as at the stage of plateau of fibril formation. They consisted of segments, whose sizes including the height along the *z*-axis and molecular volumes were similar to individual tetra- and octamers in the same sample. Formation of rings during the incubation period was a stochastic process; their population varied substantially under equivalent conditions, or they can be completely absent. No correlation was found with protein concentration or with distinct type population of oligomers.

The AFM analysis was carried out just after the transfer of amyloid from the incubation buffer to the serum-free medium, as well as after their 48 h incubation in culture medium in the presence or absence of IMR-32 cells at 37°C. Both morphology and size of oligomers, fibrils, and amyloid rings measured at cross-sections were unchanged under all these conditions. Larger amorphous aggregates appeared in the inspected solutions along with amyloid structures. Amorphous aggregation was also observed in the solution of monomeric lysozyme in the course of the same incubation range in serum-free medium; however, further studies showed non-toxicity of these aggregates. Thus the data confirmed that once formed, amyloid structures of horse lysozyme remain stable under the conditions of experiments on cytotoxicity, including the fact that the cells present had no influence on their morphology.

Influence of amyloid on viability of cells determined by ethidium bromide staining. Three cell types—primary neuronal cells, primary fibroblasts, and neuroblastoma cell line IMR-32—were used in experiments on the influence of amyloid structures on cell viability. Their viability was evaluated by the extent of staining with ethidium bromide as described above. The results of measurements are given on Figs. 4 and 5. Identical additions of incubation buffer and freshly dissolved monomeric lysozyme employed as negative controls did not influence the cell viability (Fig. 4). Protofilaments obtained after 12-24 days of incubation at pH 2.0 as well as at pH 4.5 were nontoxic at concentration ranging from 5 to 50 μM; under our experimental conditions, they did not induce cell death even in the most sensitive primary neuronal cells (Fig. 4). However, the amyloid oligomers corresponding to the growth phase on the kinetic curve of fibril formation (Fig. 2) and observed by AFM did induce cell death in all cell types employed in our experiments. A prominent dependence of cell viability on concentration of added amyloid was observed: the percentage of dead cells increased with elevation of amyloid oligomer concentration. The maximum cytotoxic effect was characteristic of oligomers formed at pH 4.5 in comparison with the structures formed at pH 2.0. Primary neuronal cells were the most sensitive to amyloid oligomer structures obtained in the solution at pH 4.5. Their mortality at lysozyme concentration of 50 μM reached 48%, whereas the death of primary fibroblasts and the cells of the line IMR-32 with the same additions of amyloid solutions was 38 and 12%, respectively (Fig. 5, a-c). The cell mortality in all inspected cell lines did not exceed 15% when oligomers formed at pH 2.0 (Fig. 2) were added at protein concentration of even 50 μM.

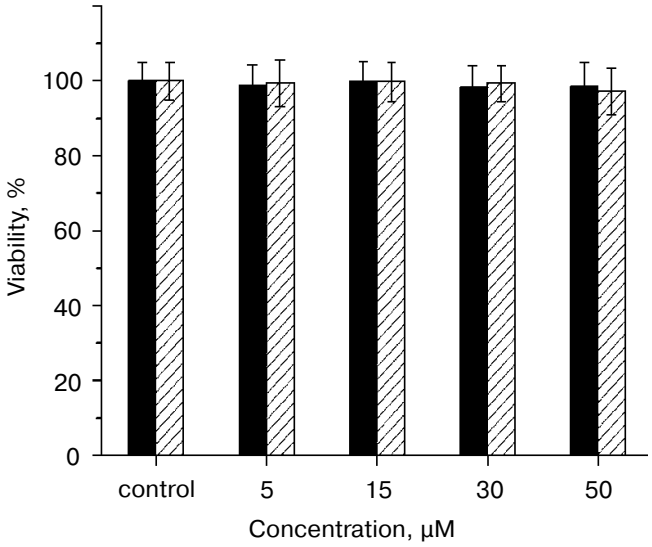

Fig. 4. Absence of cytotoxic effect of horse lysozyme fibrillar structures obtained as a result of incubation either at pH 4.5, 57°C (black columns), or at pH 2.0 and 57°C (hatched columns) on primary neuronal cells. The abscissa (*x*-axis) is the concentration of protein added to the cells. The percentage of viability evaluated by the extent of staining of the cells with ethidium bromide is shown along the *y*-axis.

DISCUSSION

We have shown that only amyloid oligomers of distinct size possess cytotoxic properties inducing cell death in all three cell types used in our experiments. Neither monomer of freshly dissolved lysozyme nor protofilaments influenced cell viability. Oligomer size depended on both medium pH and incubation time. The largest oligomers formed at pH 2.0 were tetramers and octamers, whereas the formation of larger structures corresponding to 20-mers was observed when incubated in the medium at pH 4.5. The sample containing these higher molecular weight structures possessed significantly increased cytotoxic properties. Since both samples are characterized by identical ability to bind the amyloid dye thioflavin T, one may anticipate that they contain equal amounts of β-sheeted structures possessing specific affinity to this dye. Thus, it is oligomer size that is the crucial factor determining their cytotoxicity. The latter possibly is due to their membrane-penetrating ability depending on oligomer size and total surface hydrophobicity [30].

It is notable that among the three cell species, the primary neuronal cells proved to be the most sensitive to toxic effect of lysozyme amyloid oligomers. Selective neu-

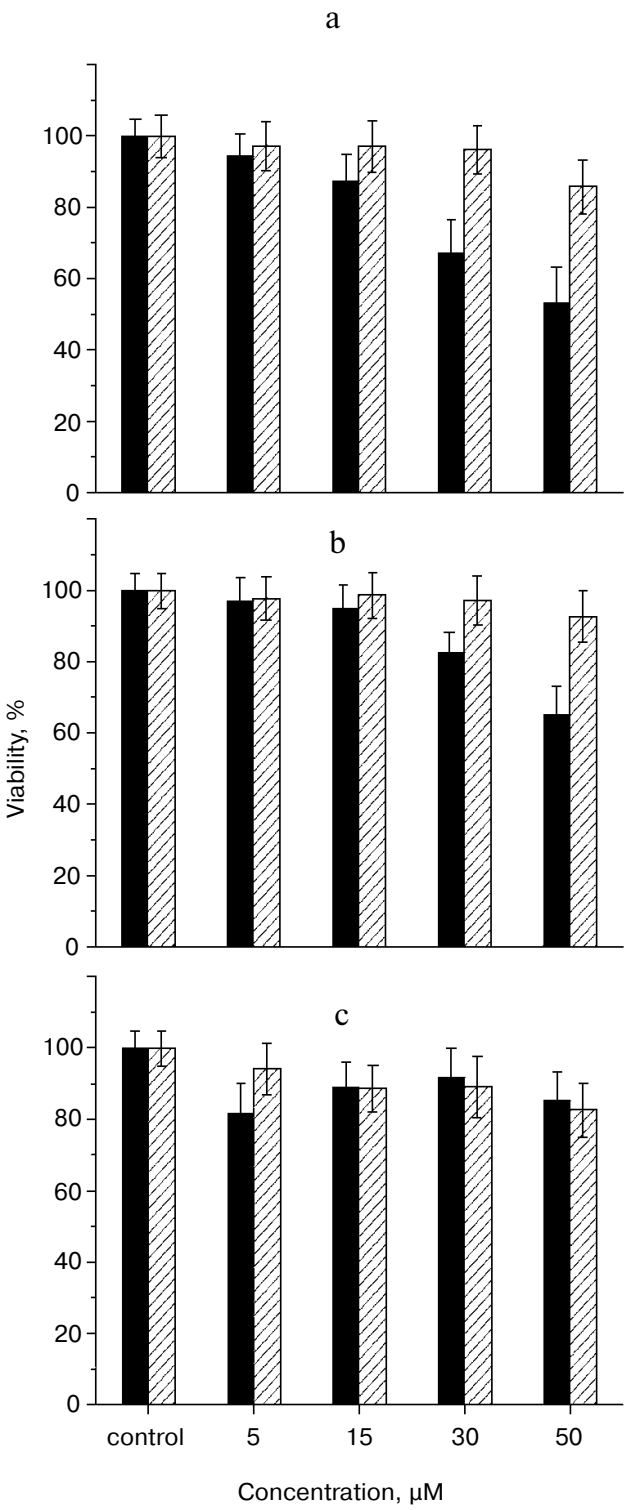

Fig. 5. Effect of amyloid oligomers on viability of primary neuronal culture (a), primary fibroblasts (b), and IMR-32 cell line (c). Black columns show the effect of oligomers obtained at pH 4.5, 57°C; hatched columns correspond to the influence of oligomers formed at pH 2.0 and 57°C. The abscissa (*x*-axis) is the concentration of protein added to the cells. The percentage of viability evaluated by the extent of staining of the cells with ethidium bromide is shown along the *y*-axis.

ronal death *in vitro* under the action of amyloid oligomers of Aβ peptide inducing Alzheimer's disease was described earlier [31]. However, in comparison with ring structures of Aβ peptide and α-synuclein playing the key role as the most toxic components in pathogeneses of Alzheimer's and Parkinson's diseases [23], no dependence between the number of rings present in the sample of horse lysozyme and cytotoxic effect of the sample was observed. Analysis of amyloid rings of lysozyme by AFM showed that they consist of segments similar in size to individual oligomers present in the same sample. Similar morphology of amyloid rings was observed in amyloid samples of the artificial protein albebetin, in which the segmentation of rings was apparently due to association of individual oligomers [32]. The ability of lysozyme amyloid to associate into rings depends on the concentration of calcium ions in the culture medium and the pH of the solution [22]. It is obvious, however, that cytotoxicity of lysozyme sample is not determined by ability of oligomers to self-assemble into rings, but depends on their actual size.

Lysozyme occupies a prominent place among amyloidogenic proteins described to date due to its wide distribution and presence in a variety of organisms and foodstuffs. The fact that it forms toxic amyloid oligomers confirms the hypothesis on common amyloidogeneity of polypeptide chain [11]. Since lysozyme can be found under a very wide range of conditions *in vivo* and *in vitro*, some of these conditions can provoke its spontaneous assembling into toxic oligomers. Since only the structures of distinct type possess toxicity and this effect can be exhibited only on distinct cell types, such as neuronal cells, for example, the frequency of amyloid toxicity occurrence under *in vivo* conditions may be not high. Moreover, we have shown recently that oligomeric and prefibrillar structures of the Alzheimer's disease marker Aβ peptide, as well as lysozyme, are excreted from the patient's body via the immune system at early stages of Alzheimer's disease [33]. These observations emphasize the important role of the immune system in the prevention of amyloidosis development, as well as the fact that formation of amyloid oligomers of various protein nature can serve as a tracer of the disease initiation. However, purposeful shift of equilibrium to the formation of toxic oligomeric structures under controlled conditions may have therapeutic effect, as in the case of amyloid oligomers of human α-lactalbumin employed for elimination of cancer cells [12]. Thus, soluble amyloid oligomers can serve as therapeutics as well as tracers of disease development. In the latter case, the block of their formation and opportune elimination from the body is one of the main ways of disease prevention.

This work was performed with the financial support of the Russian Academy of Sciences (the program for Molecular and Cellular Biology), grant No. RI-112/001/200, and the Swedish Medical Research Council, grant Nos. 2002-7884 and 2005-6543. Mantas Malisauskas is

grateful to the Sven and Lilli Lawskis Association for a Fellow Award. The authors are indebted to the Kempe Association for purchase of the atomic force microscope.

REFERENCES

1. Koudinova, N. V., Berezov, T. T., and Koudinov, A. R. (1999) *Biochemistry (Moscow)*, **64**, 752-757.
2. Kasumova, S. Iu. (2002) *Zh. Vopr. Neirokhir. im. N. N. Burdenko*, **4**, 45-48.
3. Rogaev, E. I. (1999) *Vestn. Ross. Akad. Med. Nauk*, No. 1, 33-39.
4. Serov, V. V. (1998) *Arkh. Patol.*, **60**, 23-27.
5. Dobson, C. M. (2003) *Nature*, **426**, 884-890.
6. Pepys, M. B., Hawkins, P. N., Booth, D. R., Vigushin, D. M., Tennent, G. A., Soutar, A. K., Totty, N., Nguyen, O., Blake, C. C., Terry, C. J., Feest, G., Zalin, A. M., and Hsuan, J. J. (1993) *Nature*, **362**, 553-557.
7. Harrison, R. F., Hawkins, P. N., Roche, W. R., MacMahon, R. F., Hubscher, S. G., and Buckels, J. A. (1996) *Gut*, **38**, 151-152.
8. Lee, K. W., Lee, S. H., Kim, H., Song, J. S., Yang, S. D., Paik, S. G., and Han, P. L. (2004) *J. Neurosci. Res.*, **76**, 572-580.
9. Gong, Y., Chang, L., Viola, K. L., Lacor, N. P., Lambert, M. P., Finch, C. E., Krafft, G. A., and Klein, W. L. (2003) *Proc. Natl. Acad. Sci. USA*, **100**, 10417-10422.
10. Andersson, K., Olofsson, A., Nielsen, E. H., Svehag, S. E., and Lundgren, E. (2002) *Biochem. Biophys. Res. Commun.*, **294**, 309-314.
11. Bucciantini, M., Giannoni, E., Chiti, F., Baroni, F., Formigli, L., Zurdo, J., Taddei, N., Ramponi, G., Dobson, C. M., and Stefani, M. (2002) *Nature*, **416**, 507-511.
12. Svensson, M., Hakansson, A., Mossberg, A. K., Linse, S., and Svanborg, C. (2000) *Proc. Natl. Acad. Sci. USA*, **97**, 4221-4226.
13. Sunde, M., Serpell, L. C., and Bartlam, M. (1997) *J. Mol. Biol.*, **273**, 729-739.
14. Sotirov, L. (2004) *Revue Med. Vet.*, **155**, 221-225.
15. Morozova, L. A., Haynie, D. T., Arico-Muendel, C., van Dael, H., and Dobson, C. M. (1995) *Nat. Struct. Biol.*, **10**, 171-175.
16. Morozova-Roche, L. A., Arico-Muendel, C., Haynie, D. T., Emelyanenko, V. I., van Dael, H., and Dobson, C. M. (1997) *J. Mol. Biol.*, **268**, 903-921.
17. Morozova-Roche, L. A., Jones, J. A., Noppe, W., and Dobson, C. M. (1999) *J. Mol. Biol.*, **289**, 1055-1073.
18. Morozova-Roche, L. A. (2002) *Doctoral dissertation (in Physics and Math)* [in Russian], ITEB RAN, Pushchino.
19. Morozova-Roche, L. A., Zurdo, J., Spencer, A., Noppe, W., Receveur, V., Archer, D. B., Joniau, M., and Dobson, C. M. (2000) *J. Struct. Biol.*, **130**, 339-351.
20. Krebs, M., Morozova-Roche, L. A., Daniel, K. A., Robinson, C. V., and Dobson, C. M. (2004) *Protein Sci.*, **13**, 1933-1938.
21. Goers, J., Permyakov, S. E., Permyakov, E. A., Uversky, V. N., and Fink, A. L. (2002) *Biochemistry*, **41**, 12546-12551.
22. Malisauskas, M., Zamotin, V., Jass, J., Noppe, W., Dobson, C. M., and Morozova-Roche, L. A. (2003) *J. Mol. Biol.*, **330**, 879-890.
23. Lashuel, H. A., Hartley, D., Petre, B. M., Walz, T., and Lansbury, P. T., Jr. (2002) *Nature*, **418**, 291.
24. Noppe, W., Hanssens, I., and De Cuyper, M. (1996) *J. Chromatogr. A*, **719**, 327-331.
25. Levine, H. (1995) *Amyloid*, **2**, 1-6.
26. Schneider, S. W., Larmer, J., Henderson, R. M., and Oberleithner, H. (1998) *Pflugers Arch.*, **435**, 362-367.
27. Geisse, N. A., Wasle, B., Saslowsky, D. E., Henderson, R. M., and Edwardson, J. M. (2002) *J. Membr. Biol.*, **189**, 83-92.
28. Dorman, D. C., Bolon, B., and Morgan, K. T. (1993) *Toxicol. Appl. Pharmacol.*, **122**, 265-272.
29. Piras, G., El Kharroubi, A., Kozlov, S., Escalante-Alcalde, D., Hernandez, L., Copeland, N. G., Gilbert, D. J., Jenkins, N. A., and Stewart, C. (2000) *Mol. Cell. Biol.*, **20**, 3308-3315.
30. Alberts, B., Lewis, J., Raff, R., Roberts, K., and Watson, J. D. (1994) *Molecular Biology of the Cell*, 3rd Edn., Garland Publishing, USA.
31. Kim, H. J., Chae, S. C., Lee, D. K., Chromy, B., Lee, S. C., Park, Y. C., Klein, W. L., Krafft, G. A., and Hong, S. T. (2003) *FASEB J.*, **17**, 118-120.
32. Lavrikova, M. A., Zamotin, V., Malisauskas, M., Chertkova, R., Kostanyan, I. A., Dolgikh, D. A., Kirpichnikov, M. P., and Morozova-Roche, L. A. (2006) *Biochemistry (Moscow)*, **71**, 306-314.
33. Gruden, M. A., Davudova, T. B., Malisauskas, M., Zamotin, V. V., Sewell, R. D. E., Voskresenskaya, N. I., Kostanyan, I. A., Sherstneva, V. V., and Morozova-Roche, L. A. (2004) *Dement. Geriatr. Cogn. Disord.*, **18**, 165-171.